Published in final edited form as:
*Mol Cell Neurosci*. 2014 September ; 62: 42–50. doi:10.1016/j.mcn.2014.08.003.

# N-Myristoylation regulates the axonal distribution of the fragile X-related protein FXR2P

**Emily E. Stackpole**[1], **Michael R. Akins**[1,2], and **Justin R. Fallon**[1]

[1]Department of Neuroscience, Brown University, Providence, RI 02912 USA

[2]Department of Biology, Drexel University, Philadelphia, PA 19104 USA

## Abstract

Fragile X Syndrome, the leading cause of inherited intellectual disability and autism, is caused by loss of function of Fragile X mental retardation protein (FMRP). FMRP is an RNA binding protein that regulates local protein synthesis in the somatodendritic compartment. However, emerging evidence also indicates important roles for FMRP in axonal and presynaptic function. In particular, FMRP and its homolog FXR2P localize axonally and presynaptically to discrete endogenous structures in the brain termed Fragile X granules (FXGs). FXR2P is a component of all FXGs and is necessary for the axonal and presynaptic localization of FMRP to these structures. We therefore sought to identify and characterize structural features of FXR2P that regulate its axonal localization. Sequence analysis reveals that FXR2P harbors a consensus N-terminal myristoylation sequence (*MGXXXS*) that is absent in FMRP. Using click chemistry with wild type and an unmyristoylatable G2A mutant we demonstrate that FXR2P is N-myristoylated on glycine 2, establishing it as a lipid-modified RNA binding protein. To investigate the role of FXR2P N-myristoylation in neurons we generated fluorescently tagged wild type and unmyristoylatable FXR2P (WT and G2A, respectively) and expressed them in primary cortical cultures. Both $FXR2P^{WT}$ and $FXR2P^{G2A}$ are expressed at equivalent overall levels and are capable of forming FMRP-containing axonal granules. However, $FXR2P^{WT}$ granules are largely restricted to proximal axonal segments while granules formed with unmyristoylatable $FXR2P^{G2A}$ are localized throughout the axonal arbor, including in growth cones. These studies indicate that N-terminal myristoylation of the RNA binding protein FXR2P regulates its localization within the axonal arbor. Moreover, since FMRP localization within axonal domains requires its association with FXR2P, these findings suggest that FXR2P lipid modification is a control point for the axonal and presynaptic distribution of FMRP.



Correspondence to: Justin R. Fallon, Department of Neuroscience, Brown University, Box G-LN, Providence, RI 02912 USA, Phone: 401-863-9308, Fax: 401-863-1074, Justin_Fallon@brown.edu.

**Role of Authors:** All authors had full access to all the data in the study and take responsibility for the integrity of the data and the accuracy of the data analysis. Study concept and design: EES, MRA and JRF. Acquisition of data: EES. Analysis and interpretation of data: EES, MRA and JRF. Drafting of the manuscript: EES and JRF. Critical revision of the manuscript for intellectual content: EES, MRA and JRF. Obtained funding: MRA and JRF.

**Keywords**

RNA binding proteins; myristoylation; Fragile X syndrome; FXR2P

## INTRODUCTION

Fragile X Syndrome (FXS) is the leading cause of inherited intellectual disability and autism (Pickett and London, 2005; Cohen et al., 2005; Hernandez et al., 2009). Individuals with FXS typically present with variable degrees of intellectual impairment, hyperactivity, anxiety and seizures (Garber et al., 2008). In addition, essentially all FXS patients demonstrate autistic features such as language impairments, social anxiety, and inappropriate emotional responses (Hernandez et al., 2009). FXS is almost always caused by the transcriptional silencing of the Fragile X mental retardation gene *FMR1*, resulting in the loss of its protein product, the RNA binding protein FMRP (Siomi et al., 1993).

Investigations of FMRP function have largely focused on its role in the somatodendritic compartment, where it regulates protein synthesis and influences synaptic plasticity (Bear et al., 2004; Bagni and Greenough, 2005; Bassell and Warren, 2008). However, FMRP is also localized to axonal and presynaptic sites in both cultured neurons and the intact brain (Feng et al., 1997a; Antar et al., 2006; Price et al., 2006; Christie et al., 2009; Till et al., 2010; Akins et al., 2012). Several lines of evidence indicate that FMRP has important roles in these axonal and presynaptic domains. Enduring synaptic plasticity in *Aplysia* neurons requires both postsynaptic and presynaptic FMRP (Till et al., 2010). In *Drosophila,* FMRP controls axonal arborization as well as presynaptic function and structure in an activity-dependent manner, possibly in part through local regulation of *dscam* translation (Zhang et al., 2001; Tessier and Broadie, 2008; Cvetkovska et al., 2013; Kim et al., 2013). In mammals, FMRP in the presynaptic neuron is required for synapse formation, synaptic activity and presynaptic short-term plasticity (Hanson and Madison 2007; Deng et al., 2011; Deng et al., 2013; Ferron et al., 2014). Finally, axonal and presynaptic FMRP is poised to function as a translational regulator since FMRP binds mRNAs that encode approximately one-third of the presynaptic proteome (Darnell et al. 2011).

Previous work from our laboratory has shown that in the intact brain FMRP and its homologs FXR1P and FXR2P localize to endogenous axonal and presynaptic granules termed FXGs (Fragile X granules; Christie et al., 2009; Akins et al., 2012). These granules are expressed within a restricted subset of neurons throughout the mammalian brain including corticocortical and thalamacortical fibers, olfactory sensory neuron axons, hippocampal CA3 associational axons and cerebellar parallel fibers (Akins et al., 2012). FXR2P is a component of all FXGs, while FMRP and FXR1P are only detected in a circuit-selective subset (Christie et al., 2009). Moreover, FXR2P, but not FMRP, is required for FXG expression (Christie et al., 2009). Taken together, these studies indicate that FXR2P is a key regulator of both FXG expression and the axonal and presynaptic localization of FMRP.

Here we sought to characterize the mechanisms that regulate the axonal distribution of FXR2P. Database searches revealed that FXR2P is the only Fragile X protein family

member that contains a consensus N-terminal myristoylation motif (*MGXXXS*). N-myristoylation is the covalent attachment of myristate, a 14-carbon saturated fatty acid, to the N-terminal glycine (G2). This irreversible fatty-acid modification occurs co-translationally following the removal of initiator methionine residues (Wilcox et al., 1987; Towler et al., 1987). N-myristoylation is observed in a wide range of proteins including src family kinases, protein kinase A, NAP-22, MARCKS and rapsyn (Resh, 1994; Carr et al., 1982; Takasaki et al., 1999; Aderem et al., 1988; James and Olson, 1989; Musil et al., 1988). The primary function of myristoylation is to regulate protein targeting by promoting interactions with the plasma membrane, lipid microdomains or hydrophobic pockets of other proteins (Taniguchi, 1999; Resh, 2004; Sorek et al., 2009).

Here we demonstrate that FXR2P is N-terminally myristoylated by virtue of its second glycine. We utilized a cultured neuron system to assess the role of N-myristoylation for FXR2P localization in axons. While both wild type and unmyristoylatable FXR2P form axonal granules containing FMRP, these forms show strikingly different localization within the axonal arbor. Granules containing wild type FXR2P are largely restricted to the proximal domain of the axonal arbor, while granules formed from mutant FXR2P invade the entire axon arbor including the growth cone. Taken together, these results show that N-terminal myristoylation regulates the localization of the RNA binding protein FXR2P within the axonal arbor.

## RESULTS

### FXR2P contains a consensus N-myristoylation motif

Since FXR2P is the only Fragile X family member required for FXG expression, we performed database analyses to search for features unique to this protein. As shown in Fig. 1A, we observed that the N-termini of all mammalian FXR2P sequences queried contain a consensus N-terminal myristoylation sequence (*MGXXXS*). This sequence is not present in any FMRP or FXR1P sequences analyzed. It is also absent in dFMRP, the sole member of the Fragile X protein family in *Drosophila*.

### FXR2P is N-terminally myristoylated

N-myristoylation is the covalent attachment of a myristoyl moiety to the glycine at the second position (G2) after removal of the initiator methionine. We used a bio-orthogonal labeling approach to test whether the N-terminal *MGXXXS* motif confers FXR2P myristoylation. In this method, proteins are metabolically labeled with a biotinylatable myristic acid analog, immunopurified, and then biotinylated *in vitro* using click chemistry (Fig. 1B; Heal et al., 2011). Polypeptides with a covalently attached myristic acid analog are thus biotinylated. COS-7 cells were transfected with either wild type FXR2P ($FXR2P^{WT}$) or a G2A mutant predicted to be unmyristoylatable ($FXR2P^{G2A}$) and then incubated with the myristic acid analog. As shown in Fig. 1C, analysis of the immunoprecipitates following the click reaction showed that $FXR2P^{WT}$ is N-myristoylated. In contrast, $FXR2P^{G2A}$ was not biotinylated, indicating that glycine-2 is necessary for FXR2P myristoylation.

We performed several controls to confirm the specificity of this finding (Fig. 1C). 1) Western blotting with anti-FXR2P showed that both $FXR2P^{WT}$ and $FXR2P^{G2A}$ were expressed and immunoprecipitated with comparable efficiency. 2) The immunoprecipitation was specific as no FXR2P was detected when normal IgG was used. 3) $FXR2P^{WT}$ was only biotinylated following the click reaction, indicating that the signal was due to the incorporation of the myristic acid analog rather than endogenous biotinylation. Taken together, these experiments demonstrate that the N-terminal *MGXXXS* sequence confers FXR2P myristoylation and that glycine-2 is the site of this modification. Thus, FXR2P is a lipid-modified RNA binding protein.

## EGFP-FXR2P expression in primary neurons

To probe the function of FXR2P myristoylation in neurons, we developed a cell culture model. Primary cortical neuron cultures were grown for 3 days *in vitro* (DIV) and then co-transfected with TdTomato and either wild type or unmyristoylatable EGFP-FXR2P (EGFP-$FXR2P^{WT}$ or EGFP-$FXR2P^{G2A}$, respectively). TdTomato served as a diffusible cell fill to allow visualization of the full extent of the dendritic and axonal arbors of individual cells. Neurons transfected with either EGFP-FXR2P elaborated extensive axonal arbors and expressed either FXR2P form at equivalent levels (see below). Further, there was no detectable loss of transfected neurons up to four weeks in culture (data not shown).

We next assessed the axonal morphology of neurons expressing wild type or unmyristoylatable EGFP-FXR2P. Axonal arbors were reconstructed from TdTomato-filled neurons co-expressing either wild type or mutant FXR2P. We then measured a variety of morphological features including total axon length, number of branch points and number of terminal branches. As shown in Figure 2A–C, we observed no significant difference in any of these axonal arbor attributes in neurons expressing EGFP-$FXR2P^{WT}$ or EGFP-$FXR2P^{G2A}$ (length: 50.8mm ± 6.3 or 49.5 ± 10.4, $p = 0.9$; branch points: 38 ± 6 or 35 ± 7, $p = 0.8$; terminal branches: 40 ± 6 or 37 ± 7, $p = 0.7$; all values WT or G2A, respectively; two-tailed t test, mean ± SEM). Taken together, these findings indicate that the cell viability and overall morphology of the axonal arbor are similar in neurons expressing either wild type or mutant EGFP-FXR2P.

## EGFP-FXR2P forms granules within axons

FXR2P is essential for the expression of FXGs, which are endogenous granules localized to axons of the intact brain (Christie et al., 2009; Akins et al., 2012). We therefore used our cultured neuron system to ask whether N-myristoylation of FXR2P plays a role in granule formation within axons. As shown in Figure 3, EGFP-$FXR2P^{WT}$ formed discrete granular structures in axons of cultured cortical neurons. These axonal EGFP-FXR2P granules were observed from the earliest time point examined (DIV6). EGFP-$FXR2P^{G2A}$ also formed axonal granules whose structure was indistinguishable from those comprised of EGFP-$FXR2P^{WT}$ (Fig. 3C, D). Further, granules formed from both wild type and unmyristoylatable EGFP-FXR2P readily associated with endogenous FMRP, with no obvious difference in FMRP colocalization between FXR2P types (Fig. 3B, D). Similar results were observed in neurons examined at DIV10 and DIV14 (data not shown). Thus

EGFP-FXR2P forms axonal granules and associates with FMRP within these structures independently of N-myristoylation.

### N-myristoylation regulates the distribution of FXR2P granules within the axonal arbor

FXGs in the intact rodent brain are present throughout the entire axonal arbor, as much as tens of millimeters from the cell body (Christie et al., 2009; Akins et al, 2012). We thus asked whether N-myristoylation might regulate the distribution of FXR2P granules within axons. For these experiments we adjusted the transfection efficiency to allow for reconstruction of the entire axonal arbors of individual neurons. As shown in Figure 4, we observed striking differences between the axonal distributions of granules formed from wild type as compared to unmyristoylatable EGFP-FXR2P. EGFP-FXR2P$^{WT}$ granules were largely restricted to proximal axonal segments (<2000 μm from cell soma) and were infrequently observed in distal axons or growth cones (Fig. 4A–G). In contrast, EGFP-FXR2P$^{G2A}$ granules invaded the full extent of the axonal arbor and were also observed in growth cones (Fig. 4H–N). As shown in Figure 4O, there was no detectable difference in the total number of axonal granules between neurons expressing either EGFP-FXR2P$^{WT}$ or EGFP-FXR2P$^{G2A}$. However, the distal axon contained five-fold more EGFP-FXR2P$^{G2A}$ granules compared to EGFP-FXR2P$^{WT}$ (0.8 ± 0.3 or 4 ± 1, for WT and G2A, respectively; mean ± SEM; $p < 0.05$; Fig. 4Q). In contrast, there was no significant difference in the number of FXR2P granules within proximal axonal segments (36 ± 6 or 48 ± 13 for WT and G2A, respectively; Fig. 4P).

We considered that the increased localization of EGFP-FXR2P$^{G2A}$ granules in the distal axonal arbor might reflect differences between the overall expression of EGFP-FXR2P$^{G2A}$ and EGFP-FXR2P$^{WT}$. To test this possibility, we performed Western blotting to compare the total levels of wild type and unmyristoylatable EGFP-FXR2P in the transfected cultures. As shown in Figure 4R, the expression of EGFP-FXR2P$^{WT}$ and EGFP-FXR2P$^{G2A}$ were indistinguishable. These observations, taken together with the finding that the length and overall complexity of the axonal arbors are comparable in neurons expressing either construct (Fig. 2), indicate that N-myristoylation regulates the distribution of FXR2P in the axon.

## DISCUSSION

In this study we demonstrate that the RNA binding protein FXR2P is N-myristoylated and that this modification regulates its distribution within the axonal arbor. Here we discuss the potential functions of FXR2P myristoylation and its implications for local protein synthesis in axons.

FXR2P is unique amongst the Fragile X protein family in containing a consensus N-terminal myristoylation motif (*MGXXXS*). This motif is highly conserved in mammalian FXR2P and is absent in FMRP and FXR1P, the other members of the vertebrate Fragile X family (Fig. 1). This site is also lacking in dFMRP, the sole Fragile X homolog present in *Drosophila*. We used a bio-orthogonal labeling method to demonstrate that FXR2P can be myristoylated. This conclusion was supported by a series of immunological, biochemical and genetic controls (Fig. 1). In accord with the established mechanism of N-myristoylation, this lipid

modification within FXR2P requires the glycine residue in position 2 (G2A mutant; Towler et al., 1987). Taken together, these results show that FXR2P is the sole member of the Fragile X family that can be myristoylated.

Our work further demonstrates that N-myristoylation regulates the distribution of FXR2P within axonal arbors. Granules formed from unmyristoylatable FXR2P are five times more abundant in the distal axon compared to wild type (Fig. 4Q). In contrast, there was no difference in the number of granules formed from either wild type or mutant FXR2P in the proximal axon segment (Fig. 4P). Several observation indicate that this differential distribution is due to myristoylation and is not a consequence of the transfection system used: 1) the expression of either EGFP-tagged wild type or mutant FXR2P in primary neurons was well tolerated with no indications of gross defects in neuronal morphology (Fig. 2); 2) the overall expression levels of EGFP-tagged wild type and mutant FXR2P were comparable (Fig. 4R); 3) neurons expressing either FXR2P form were viable for up to 28 days following transfection; 4) the morphology of the axonal arbors was indistinguishable between neurons expressing either wild type or mutant FXR2P (Fig. 2); and 5) as observed for other RNA binding proteins expressed in neurons, both wild type and mutant FXR2P formed granules (Figs. 3, 4; Köhrmann et al., 1999; Davidovic et al., 2007; Levenga et al., 2009). Taken together, these results indicate that myristoylation is important for regulating FXR2P localization within the axonal arbor.

A targeting role for FXR2P myristoylation is in accord with studies of other proteins subject to this lipid modification. The addition of lipid moieties, including myristoyl groups, regulates protein localization to a variety of cellular domains and subdomains (Resh, 2004). Myristoylation directs proteins to hydrophobic environments ranging from specific protein binding domains or specialized vesicle structures to generalized regions within the plasma membrane, including neuronal processes (O'Callaghan et al., 2003; Spilker et al., 2002; Takasaki et al., 1999; Resh, 2004; Taniguchi, 1999). Thus, myristoylation could serve to actively restrict FXR2P localization in the axonal arbor by promoting interactions with either a protein binding partner or a lipid domain that is enriched in the proximal region of the axon. The mechanism and targets of such a myristoylation-dependent FXR2P binding partner are currently unknown.

Our results suggest two mechanisms by which myristoylation might selectively regulate FXR2P localization within the axonal arbor. Myristoylation is a co-translational process where a myristoyl moiety is irreversibly attached to the N-terminal glycine (Towler et al., 1987; Wilcox et al., 1987). In the simplest model, neurons may endogenously synthesize both myristoylated and unmyristoylated forms of FXR2P. In this case, the extent of FXR2P distribution within the axonal arbor would be a function of the relative expression levels of the myristoylated and unmyristoylated forms. In this co-translational model, such differential lipid modification could be regulated at either the level of the N-myristoyltransferases that catalyze myristoyl group addition to the N-terminal glycine (Towler et al., 1988) or the methionine aminopeptidases that cleave the N-terminal methionine (Frottin et al., 2006).

Myristoylation could also act as part of a posttranslational switch to regulate FXR2P localization within the axonal arbor. In this model, FXR2P in both the distal and proximal axons may be myristoylated, but exist in different post-translational states. Work in other systems has shown that myristoylation confers only weak hydrophobic associations that can be overridden by factors such as phosphorylation and conformational changes (Zozulya and Stryer, 1992; Peitzsch and McLaughlin, 1993; Taniguchi, 1999). For example, phosphorylation regulates the partitioning of myristoylated MARCKS protein between the plasma membrane and F-actin (Blackshear et al., 1993). Moreover, calcium binding to the myristoylated protein hippocalcin causes a conformational change that promotes its translocation to the postsynaptic membrane (Palmer et al., 2005). Interestingly, hippocalcin can also recruit AP2 (adaptor protein 2) to the membrane, suggesting that myristoylated proteins can direct the movement of associated proteins to specific subcellular domains (Palmer et al., 2005). A posttranslational switch collaborating with myristoylation to regulate FXR2P localization is highly attractive as it provides a reversible mechanism for the local regulation of FXR2P dynamics within the axonal arbor. Such an FXR2P switch could be a target of neuronal activity and/or interactions with the local environment.

Myristoylation-dependent FXR2P localization could also regulate protein synthesis within the axonal arbor. RNA binding proteins are key components of local translation – acting as targeting molecules localizing mRNA to distinct domains and subsequently regulating translation locally at these remote sites (Bramham and Wells, 2007; Kiebler and Bassell, 2006; Kapeli and Yeo, 2012; Darnell, 2013). Therefore, important regulators of local translation are the molecular mechanisms that spatially restrict RNA binding proteins to specific subdomains within cells. As myristoylation promotes association with both membranes and hydrophobic pockets within proteins, this lipid modification could offer select RNA binding proteins – including FXR2P – a unique method for cellular localization. This study demonstrates that myristoylation inhibits the localization of FXR2P from both axonal growth cones and distal axonal arbors, thereby acting as a potential means to spatially control local translation within the axonal domain. Thus, the addition of a myristoyl moiety to FXR2P and potentially other as yet unidentified RNA binding proteins could contribute in part to translational control within neurons.

Finally, these results have implications for FMRP function within the brain. FXGs (Fragile X granules) are endogenous axonal granules in the intact brain that contain both FXR2P and FMRP (Christie et al., 2009; Akins et al., 2012). Notably, FMRP localizes to FXGs by virtue of its association with FXR2P. Thus changes in FXR2P localization in axons would affect FMRP distribution in this compartment as well. Our findings that N-myristoylation regulates the axonal distribution of FXR2P therefore raise the possibility that FMRP localization would likewise be affected. Importantly, we also show that FMRP association with FXR2P is independent of this lipid modification: both EGFP-tagged wild type and unmyristoylatable FXR2P granules readily contained FMRP (Fig. 3B, D). Together, our results suggest that N-myristoylation of FXR2P regulates FMRP distribution within the brain. As such, FXR2P N-myristoylation could regulate FMRP-dependent axonal and presynaptic functions. Future *in vivo* experiments should address the contribution of FXR2P N-myristoylation to the axonal localization of FXGs and the roles this modification might play in regulating local axonal and presynaptic translation in the brain.

## MATERIALS AND METHODS

### Plasmids

Full-length *fxr2* was generated from an *fxr2* clone (Open Biosystems; MMM1013-9498022) by PCR and subcloned into either the pBluescriptKSII or pCAGES vector. EGFP-FXR2P was produced by insertion of the EGFP sequence at amino acid 217 via a transposition reaction (Sheridan et al., 2002) using the modified Tn5 transposon encoding *EGFP-Kan$^R$-STOP* (pBNJ24.6; a kind gift of Dr. Thomas Hughes). An unmyristoylatable form of FXR2P was generated by PCR using the primer 5′ – ACCGGTATGGCAGGCCTGGCC – 3′. The modified pCAG vector (pCAGES) was generated by first subcloning out EGFP from the pCAG-EGFP vector and inserting blunted oligonucleotides containing a new multiple cloning site (forward: 5′-AATTCGATATCACCGGTATCGATGCTAGCGAGCTCGCGGCCGCCTCGAGCAGCT G GGTAC-3′ and reverse: 3′-CCAGCTGCTCGAGGCGGCCGCGAGCTCGCTAGCATCGATACCGGTGATATCG-5′) into the EcoRI and KpnI overhanging sites. A plasmid containing TdTomato under the control of the chicken *beta-actin* promoter was generated by restriction subcloning TdTomato from the pTRE-Bi-SG-T plasmid (Addgene, Cambridge, MA) into the pCAGES vector. The structure of all constructs was confirmed by sequencing.

### Transfection and Metabolic Labeling

COS-7 cells were transfected with untagged wild type FXR2P or unmyristoylatable mutant FXR2P-G2A using FugeneHD (Promega, Madison, WI) according to the manufacturer's instructions. One hour after transfection, cells were treated with 50 μM myristic acid alkyne (Cayman Chemical; Ann Arbor, MI), which was allowed to incorporate into newly synthesized proteins for 23 hrs. Cells were then washed twice with cold PBS and incubated with Triton-X lysis buffer (50 mM Tris pH 7.5, 150 mM sodium chloride, 5 mM EDTA, 1% Triton X-100, 2 mM sodium orthovanadate, 10 mM β-glycerophosphate, 1X protease inhibitor cocktail [Roche; United States]) for 15 mins at 4°C. Lysates were then collected and centrifuged at 10,000*g* for 15 min at 4°C.

### Immunoprecipitation and Click-iT Reaction

Lysate supernatants were precleared by incubation with 50 μL protein A Dynabeads (Invitrogen; Grand Island, NY) for 1 hr at 4°. Immunoprecipitation for FXR2P was performed with protein A Dynabeads conjugated to the rabbit polyclonal antibody BU38 (Akins et al., 2012; 10 μL antibody with 25 μL Dynabeads) for 2 hrs at 4°. As a specificity control, separate precleared lysates were simultaneously treated with protein A Dynabeads conjugated to normal rabbit IgG serum (1 μg; Sigma; St. Louis, MO) for 2 hrs at 4°. After a 2 hr incubation, the flowthrough was removed and kept on ice for Western analysis while the Dynabeads were washed three times for 5 min each with Triton X-100 lysis buffer. Following the last wash, 10% of the beads in wash buffer were removed for Western analysis. The remaining 90% of beads were used for the click-iT reaction using the click-iT protein reaction kit (Invitrogen; Grand Island, NY) following the manufacturer's instructions using 40 μM biotin azide (Invitrogen; Grand Island, NY). Biotin clicked immunoprecipitates were washed three times for five mins each with Triton X-100 lysis buffer then boiled in

SDS-PAGE sample buffer (60 mM Tris pH 6.8, 2% SDS, 10% glycerol, 735 mM β-mercaptoethanol) to elute immunoprecipitated protein. Protein samples were separated using 10% SDS-PAGE gels and transferred to nitrocellulose membranes following standard methods.

### Western Blotting of Click-iT Reaction

For click-iT analysis with streptavidin-HRP (KPL, Gaithersburg, MD) to detect biotinylated proteins, membranes were blocked for 1 h at room temperature in wash buffer (100 mM Tris pH 7.4, 150 mM sodium chloride, 4% normal goat serum, and 0.1% Tween-20). Blots were then incubated with streptavidin-HRP diluted in wash buffer (1:10,000) at room temperature for 90 min followed by washing four times for 5 min each in wash buffer. For probing with a mouse anti-FXR2P antibody (clone 55; BD Biosciences, San Jose, CA), blots were blocked for 1 h at room temperature in 5% nonfat dried milk in wash buffer and then incubated overnight with diluted primary at 4°C (1:1,000). Blots were washed four times for 5 min each in wash buffer after primary incubation. Horseradish peroxidase (HRP)-conjugated secondary antibodies (KPL, Gaithersburg, MD) were diluted in 5% milk in wash buffer (1:2,000) and incubated at room temperature for 90 min. Blots were washed four times for 5 min each in wash buffer and signals were detected by chemiluminescence (Amersham ECL Western blotting reagents, Arlington Heights, IL).

### Primary Rat Cortical Neuron Culture Plating and Maintenance

All animal care and collection of tissue were in accordance with Brown University IACUC guidelines for care and use of laboratory animals. Primary rat cortical neuron cultures were prepared from P1 to P2 rat pups (Postnatal day 1 and 2, respectively; Sprague Dawley; Charles River, Boston, MA) using a papain dissociation system (Worthington Biochemicals, Lakewood, NJ). Rat pups were sacrificed by decapitation and cerebral cortices were dissected, cut into small pieces and collected in warmed (37°C) papain (20 U/mL) in Earle's Balanced Salt Solution (EBSS) with 1 mM L-cysteine, 0.5 mM EDTA, and 2000 U/mL DNAse. Tissue was incubated in papain for 30 min and then lightly triturated to dissociate cells. The cells were subsequently spun down by centrifugation at 300*g* for 5 min and resuspended in ovomucoid protease inhibitor (1 mg/mL) with bovine serum albumin (1 mg/mL) and DNAse in EBSS. A discontinuous density gradient was then prepared by layering the cell solution on top of ovomucoid protease inhibitor solution and centrifuged at 70*g* for 6 min. The pellet of dissociated cells was resuspended in Neurobasal Medium supplemented with 1% L-glutamax, 2% B27 and 100 units/mL penicillin - 100 μg/mL streptomycin sulfate (all from Invitrogen; Grand Island, NY). For microscopy experiments, cells were plated onto 24-well plates with poly-D-lysine (PDL; 50 μg/mL; Sigma; St. Louis, MO) and laminin (20 μg/mL; Invitrogen; Grand Island, NY) coated glass coverslips (Assistent; Germany) at a density of 80,000 cells/well. For Western blotting, cells were plated onto PDL-coated 6-well plates at a density of 300,000 cells/well. Cultures were maintained at 37° C and 5% $CO_2$.

### Transfection of Primary Cortical Neuron Cultures

At 3 days *in vitro* (DIV), cultures were co-transfected with EGFP-FXR2P constructs and TdTomato by magnetofection using NeuroMag paramagnetic nanobeads (Oz Biosciences;

France). For 24-well plates, plasmid DNA (0.5 μg total, or 0.25 μg each construct) was incubated with 1.75 μL NeuroMag beads (1 μg/μL) in 100 μL Opti-MEM (Invitrogen; Grand Island, NY) for 15 min. For evaluation of individual neurons transfection efficiency was decreased by using only 0.25 μg total plasmid DNA and 0.5 μL NeuroMag. For 6-well plates (used for western blotting), 0.75 μg of plasmid DNA was incubated with 2.62 μL of NeuroMag beads. The solution was then added drop-wise to cultures and allowed to incubate for 15 min on top a magnetic plate at 37°C.

### Western Blotting of Transfected Cultured Neurons

For testing expression levels of EGFP-FXR2P constructs, cultured cortical neurons (DIV3; n = 3 separate culture platings) were transfected as described above. Three days post transfection (DIV6), neurons were washed two times with cold PBS and incubated with RIPA lysis buffer (25 mM Tris pH 8.0, 150 mM sodium chloride, 0.1% SDS, 1% NP-40, 0.5% sodium deoxycholate, 5 mM EDTA, 2 mM sodium orthovanadate, NEB; Ipswich, MA; 10 mM β-glycerophosphate, 1X protease inhibitor cocktail, Roche; United States) for 15 min at 4°C. Lysates were then collected and centrifuged at 10,000*g* for 15 min at 4°C. Supernatants (10 μg) were separated by SDS-PAGE followed by western blotting (as described above) with anti-FXR2P (clone 55, 1:1000, BD Transduction Labs; San Jose, CA) and anti-γ-actin (1:40,000, Sigma; St. Louis, MO).

### Immunostaining

Coverslips were washed once with PBS then fixed for 15 min with 4% paraformaldehyde and 4% sucrose in PBS and thoroughly rinsed with PBS. Coverslips were treated with 10 mM sodium citrate, pH 6.0, for 30 min at 65° to improve antibody access. Coverslips were then treated with blocking solution (PBS with 0.3% Triton X-100 and 1% blocking reagent; Roche; United States) for 30 min and then incubated for 1 h in blocking solution plus primary antibodies against FMRP (2F5-1; 1:300; Gabel et al., 2004; Christie et al., 2009). Cells were then washed with PBST before incubation with blocking solution plus secondary antibodies (1:1,000; Invitrogen; Grand Island, NY). After washing with PBS, coverslips were mounted in mounting medium (NPG; 4% n-propyl-gallate, 60% glycerol, 5 mM phosphate pH 7.4, 75 mM sodium chloride). Confocal images were collected using a 63X Plan-Apochromat objective on a Zeiss LSM 510 microscope. Images were analyzed using ImageJ and Photoshop CS6 (Adobe, San Jose, CA).

### Evaluation of Axonal Granule Distribution and Axonal Arbors in Cultured Neurons

For visual evaluation of axonal EGFP-FXR2P granules, confocal images of fixed and transfected neurons were collected using a 63X Plan-Apochromat objective on a Zeiss LSM 510 microscope. Images were analyzed using ImageJ and Photoshop CS6 (Adobe, San Jose, CA).

For quantification of EGFP-FXR2P axonal granules and arborization, montages of 40X images were collected of individual neurons (DIV6) using Nikon Elements software and a Nikon Eclipse T800 microscope coupled with an Orca ER camera (Hammamatsu, Bridgewater, NJ). All images were collected blind to condition and using identical criteria. Neurons were chosen for analysis based on morphology. Only healthy neurons with a clear

single axonal projection were chosen for our analyses. Images of entire neurons were sharpened in Photoshop CS6 (Adobe) using the unsharp mask filter three times with the settings 500%, 2.5 pixels and 128 levels. This procedure, which highlights bright puncta ~3 pixels in diameter, identified a sizable fraction of FXR2P granules within axons.

Axonal arbors were reconstructed and analyzed using Neurolucida and Neuroexplorer software respectively (MBF Bioscience, Williston, VT). Axonal arbors were evaluated on the number of branch points per neuron, branch terminals per neuron and total axon length (n = 6 neurons per condition). For the quantification of the number of axonal FXR2P granules, all FXR2P puncta that overlapped with TdTomato labeled axons were identified and counted. To characterize the distribution of axonal FXR2P granules, a Sholl analysis was conducted using concentric radii of 20 μm extending from the center of the soma and the number of FXR2P puncta within each segment was identified and counted (n = 6 neurons per condition). Average axon length from cell soma was 8000 μm. Proximal axon segments were designated as less than 2000 μm from the center of the neuronal soma, while distal segments were defined as greater than 2000 μm from neuronal soma.

### Statistical Analyses

Variables for FXR2P axonal granule distribution and axonal morphology were statistically analyzed using Student's two-tailed t-test in GraphPad Prism. All data were collected and analyzed blind to experimental condition.

## Acknowledgments

We thank B. McKechnie and C. Schmiedel for technical assistance and E. Morrow for the use of the Neurolucida programs. We also thank T. Hughes for the generous gift of the pBNJ24.6 vector. Grant Support: HD052083 to JRF and MH090237 to MRA.

## References

Aderem AA, Albert KA, Keum MM, Wang JK, Greengard P, Cohn ZA. Stimulus- dependent myristoylation of a major substrate for protein kinase C. Nature. 1988; 332:362–364. [PubMed: 3352735]

Akins MR, Berk-Rauch HE, Fallon JR. Presynaptic translation: stepping out of the postsynaptic structure. Front Neural Circuits. 2009; 3:17. [PubMed: 19915727]

Akins MR, Leblanc HF, Stackpole EE, Chyung E, Fallon JR. Systematic mapping of fragile X granules in the mouse brain reveals a potential role for presynaptic FMRP in sensorimotor functions. J Comp Neurol. 2012; 520:3687–3706. [PubMed: 22522693]

Antar LN, Li C, Zhang H, Carroll RC, Bassell GJ. Local functions for FMRP in axon growth cone motility and activity-dependent regulation of filopodia and spine synapses. Mol Cell Neurosci. 2006; 32:37–48. [PubMed: 16631377]

Bagni C, Greenough WT. From mRNP trafficking to spine dysmorphogenesis: the roots of fragile X syndrome. Nat Rev Neurosci. 2005; 6:376–387. [PubMed: 15861180]

Bassell GJ, Warren ST. Fragile X syndrome: loss of local mRNA regulation alters synaptic development and function. Neuron. 2008; 60:201–214. [PubMed: 18957214]

Bear MF, Huber KM, Warren ST. The mGluR theory of fragile X mental retardation. Trends Neurosci. 2004; 27:370–377. [PubMed: 15219735]

Blackshear PJ. The MARCKS family of cellular protein kinase C substrates. J Biol Chem. 1993; 268:1501–1504. [PubMed: 8420923]

Bramham CR, Wells DG. Dendritic mRNA: transport, translation, and function. Nat Rev Neurosci. 2007; 8:776–789. [PubMed: 17848965]

Carr SA, Biemann K, Shoji S, Parmelee DC, Titani K. n-Tetradecanoyl is the NH2-terminal blocking group of the catalytic subunit of cyclic AMP-dependent protein kinase from bovine cardiac muscle. Proc Natl Acad Sci U S A. 1982; 79:6128–6131. [PubMed: 6959104]

Christie SB, Akins MR, Schwob JE, Fallon JR. The FXG: a presynaptic fragile X granule expressed in a subset of developing brain circuits. J Neurosci. 2009; 29:1512–1524.

Cohen D, Pichard N, Tordjman S, Baumann C, Burglen L, Excoffier E, Lazar G, Mazet P, Pinquier C, Verloes A, et al. Specific genetic disorders and autism: clinical contribution towards their identification. J Autism Dev Disord. 2005; 35:103–116. [PubMed: 15796126]

Cvetkovska V, Hibbert AD, Emran F, Chen BE. Overexpression of Down syndrome cell adhesion molecula impairs precise synaptic targeting. Nat Neurosci. 2013; 16:677–682. [PubMed: 23666178]

Darnell JC, Van Driesche SJ, Zhang C, Hung KY, Mele A, Fraser CE, Stone EF, Chen C, Fak JJ, Chi SW, Licatalosi DD, Richter JD, Darnell RB. FMRP stalls ribosomal translocation on mRNAs linked to synaptic function and autism. Cell. 2011; 146:247–261. [PubMed: 21784246]

Darnell RB. RNA protein interaction in neurons. Annu Rev Neurosci. 2013; 36:243–270. [PubMed: 23701460]

Davidovic L, Jaglin XH, Lepagnoi-Bestel AM, Tremblay S, Simonneau M, Bardoni B, Khandjian EW. The fragile x mental retardation protein is a molecular adaptor between the neurospecific KIF3C kinesin and dendritic RNA granules. Hum Mol Genet. 2007; 16:3047–3058. [PubMed: 17881655]

Deng PY, Sojka D, Klyachko VA. Abnormal presynaptic short-term plasticity and information processing in a mouse model of fragile X syndrome. J Neurosci. 2011; 31:10971–10982. [PubMed: 21795546]

Deng PY, Rotman Z, Blundon JA, Cho Y, Cui J, Cavalli V, Zakharenko SS, Klyachko VA. FMRP regulates neurotransmitter release and synaptic information transmission by modulating action potential duration via BK channels. Neuron. 2013; 77:696–711. [PubMed: 23439122]

Feng Y, Gutekunst CA, Eberhart DE, Yi H, Warren ST, Hersch SM. Fragile X mental retardation protein: nucleocytoplasmic shuttling and association with somatodendritic ribosomes. J Neurosci. 1997a; 17:1539–1547. [PubMed: 9030614]

Ferron L, Nieto RM, Cassidy JS, Dolphin AC. Fragile X mental retardation protein controls synaptic vesicle exocytosis by modulating N-type calcium channel density. Nat Commun. 2014; 5:3628. [PubMed: 24709664]

Frottin F, Martinez A, Peynot P, Mitra S, Holz RC, Giglione C, Meinnel T. The proteomics of N-terminal methionine cleavage. Mol Cell Proteomics. 2006; 5:2336–2349. [PubMed: 16963780]

Gabel LA, Won S, Kawai H, McKinney M, Tartakoff AM, Fallon JR. Visual experience regulates transient expression and dendritic localization of Fragile X mental retardation protein. J Neurosci. 2004; 24:10579–10583. [PubMed: 15564573]

Garber KB, Visootsak J, Warren ST. Fragile X syndrome. Eur J Hum Genet. 2008; 16:666–72. [PubMed: 18398441]

Hanson JE, Madison DV. Presynaptic FMR1 genotype influences the degree of synaptic connectivity in a mosaic mouse model of fragile X syndrome. J Neurosci. 2007; 27:4014–4018. [PubMed: 17428978]

Heal WP, Wright MH, Thinon E, Tate EW. Multifunction protein labeling via enzymatic N-terminal tagging and elaboration by click chemistry. Nat Protoc. 2011; 7:105–117. [PubMed: 22193303]

Hernandez RN, Feinberg RL, Vaurio R, Passanante NM, Thompson RE, Kaufmann WE. Autism spectrum disorder in fragile X syndrome: a longitudinal evaluation. Am J Med Genet A. 2009; 149A:1125–1137. [PubMed: 19441123]

James G, Olson EN. Myristoylation, phosphorylation and subcellular distribution of the 80-kDa protein kinase C substrate in BC3H1 myocytes. J Biol Chem. 1989; 264:20928–20933. [PubMed: 2592358]

Jung H, Yoon BC, Holt CE. Axonal mRNA localization and protein synthesis in nervous system assembly, maintenance and repair. Nat Rev Neurosci. 2012; 13:308–324. [PubMed: 22498899]

Kapeli K, Yeo GW. Genome-wide approaches to dissect the roles of RNA binding proteins in translational control: implications for neurological diseases. Front Neurosci. 201210.3389/fnins.2012.00144

Kiebler MA, Bassell GJ. Neuronal RNA granules: movers and makers. Neuron. 2006; 51:685–690. [PubMed: 16982415]

Kim JH, Wang X, Coolon R, Ye B. Dscam expression levels determine presynaptic arbor sizes in Drosophila sensory neurons. Neuron. 2013; 78:827–838. [PubMed: 23764288]

Köhrmann M, Luo M, Kaether C, DesGroseillers L, Dotti CG, Kiebler MA. Microtubule-dependent recruitment of Staufen-green fluorescent protein into large RNA-containing granules and subsequent dendritic transport in living hippocampal neurons. Mol Biol Cell. 1999; 10:2945–2953. [PubMed: 10473638]

Levenga J, Buijsen RA, Rife M, Moine H, Nelson DL, Oostra BA, Willemsen R, De Vrij FM. Ultrastructural analysis of the functional domains in FMRP using primary hippocampal neurons. Neurobiol Dis. 2009; 35:241–250. [PubMed: 19464371]

Musil LS, Carr C, Cohen JB, Merlie JP. Acetylcholine receptor-associated 43K protein contains covalently bound myristate. J Cell Biol. 1988; 107:1113–1121. [PubMed: 3417776]

O'Callaghan DW, Tepikin AV, Burgoyne RD. Dynamics and calcium sensitivity of the Ca2+/myristoyl switch protein hippocalcin in living cells. J Cell Biol. 2003; 163:715–721. [PubMed: 14638856]

Palmer CL, Lim W, Hastie PG, Toward M, Korolchuk VI, Burbridge SA, Banting G, Collingridge GL, Isaac JT, Henley JM. Hippocalcin functions as a calcium sensor in hippocampal LTD. Neuron. 2005; 47:487–494. [PubMed: 16102532]

Peitzsch RM, McLaughlin S. Binding of acylated peptides and fatty acids to phospholipid vesicles: pertinence to myristoylated proteins. Biochemistry. 1993; 32:10436–10443. [PubMed: 8399188]

Pickett J, London E. The neuropathology of autism: a review. J Neuropathol Exp Neurol. 2005; 64:925–935. [PubMed: 16254487]

Price TJ, Flores CM, Cervero F, Hargreaves KM. The RNA binding and transport proteins staufen and fragile X mental retardation protein are expressed by rat primary afferent neurons and localize to peripheral and central axons. Neuroscience. 2006; 141:2107–2116. [PubMed: 16809002]

Resh MD. Myristylation and palmitylation of Src family members: the fats of the matter. Cell. 1994; 76:411–413. [PubMed: 8313462]

Resh MD. Membrane targeting of lipid modified signal transduction proteins. Subcell Biochem. 2004; 37:217–232. [PubMed: 15376622]

Sheridan DL, Berlot CH, Robert A, Inglis FM, Jakobsdottir KB, Howe JR, Hughes TE. A new way to rapidly create function, fluorescent fusion proteins: random insertion of GFP with an in vitro transposition reaction. BMC Neurosci. 2002; 3

Siomi H, Siomi MC, Nussbaum RL, Dreyfuss G. The protein product of the fragile X gene, FMR1, has characteristics of an RNA-binding protein. Cell. 1993; 74:291–298. [PubMed: 7688265]

Sorek N, Bloch D, Yalovsky S. Protein lipid modifications in signaling and subcellular targeting. Curr Opin Plant Biol. 2009; 12:714–720. [PubMed: 19796984]

Spilker C, Dresbach T, Braunewell KH. Reversible translocation and activity- dependent localization of the calcium-myristoyl switch protein VILIP-1 to different compartments in living hippocampal neurons. J Neurosci. 2002; 22:7331–7339. [PubMed: 12196554]

Takasaki A, Hayashi N, Matsubara M, Yamauchi E, Taniguchi H. Identification of the calmodulin-binding domain of neuron-specific protein kinase C substrate protein CAP-22/NAP-2. Direct involvement of protein myristoylation in calmodulin-target protein interaction. J Biol Chem. 1999; 274:11848–11853. [PubMed: 10207003]

Tanaguchi H. Protein myristoylation in protein-lipid and protein-protein interactions. Biophys Chem. 1999; 82:129–137. [PubMed: 10631796]

Tessier CR, Broadie K. Drosophila fragile X mental retardation protein developmentally regulates activity-dependent axon pruning. Development. 2008; 135:1547–1557. [PubMed: 18321984]

Till SM, Li HL, Miniaci MC, Kandel ER, Choi YB. A presynaptic role for FMRP during protein synthesis-dependent long-term plasticity in Aplysia. Learn Mem. 2010; 18:39–48. [PubMed: 21177378]

Towler DA, Eubanks SR, Towery DS, Adams SP, Glaser L. Amino-terminal processing of proteins by N-myristoylation. Substrate specificity of N-myristoyl transferase. J Biol Chem. 1987; 262:1030–1036. [PubMed: 3100524]

Towler DA, Adams SP, Eubanks SR, Towery DS, Jackson-Machelski E, Glaser L, Gordon JI. Myristoyl CoA:protein N-myristoyltransferase activities from rat liver and yeast possess overlapping yet distinct peptide substrate specificities. J Biol Chem. 1988; 263:1784–1790. [PubMed: 3123478]

Wilcox C, Hu JS, Olson EN. Acylation of proteins with myristic acid occurs cotranslationally. Science. 1987; 27:1275–1278. [PubMed: 3685978]

Zhang YQ, Bailey AM, Matthles HJ, Renden RB, Smith MA, Speese SD, Rubin GM, Broadie K. Drosophila fragile X-related gene regulates the MAP1B homolog Futsch to control synaptic structure and function. Cell. 2001; 107:591–603. [PubMed: 11733059]

Zozulya S, Styer L. Calcium-myristoyl protein switch. Proc Natl Acad Sci USA. 1992; 89:11569–11673. [PubMed: 1454850]

## Highlights

- An N-terminal motif directs myristoylation of the RNA binding protein FXR2P
- FXR2P is the only myristoylated member of the Fragile X protein family
- Myristoylation regulates FXR2P granule distribution within axons

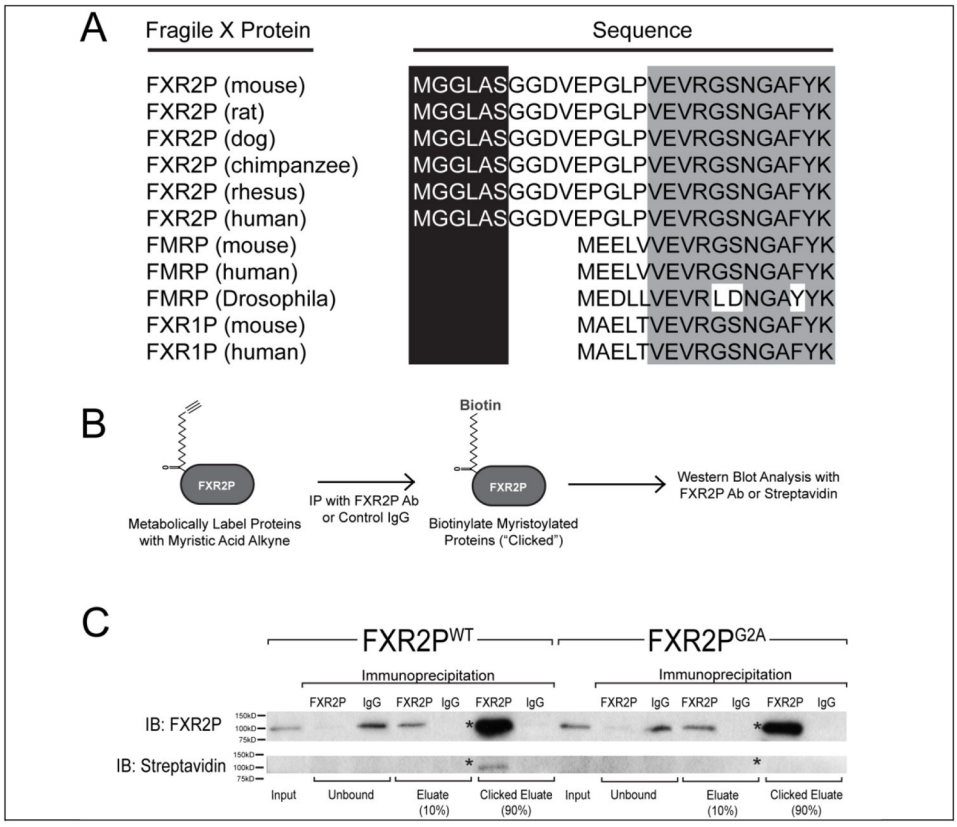


**Figure 1. FXR2P is N-terminally myristoylated**

**(A)** The N-terminus of FXR2P from the six mammalian species analyzed contains a conserved N-terminal myristoylation consensus sequence (*MGXXXS*). This consensus sequence is not present in either FMRP or FXR1P in any species examined (for clarity, only mouse, human and *Drosophila* are shown). **(B)** Schematic of click chemistry-based approach used to detect FXR2P myristoylation (see Methods). **(C)** Western blot demonstrating N-terminal myristoylation of $FXR2P^{WT}$ but not $FXR2P^{G2A}$. COS-7 cells transfected with either $FXR2P^{WT}$ or $FXR2P^{G2A}$ were incubated with a biotinylatable analog of myristic acid. Lysates were collected ('input') and then immunoprecipitated with either FXR2P antibody or a control IgG. Ninety percent of immunoprecipitates were subjected to the click-iT reaction to biotinylate proteins that had incorporated the myristic analog. Analysis of the western blots with an FXR2P antibody demonstrated the comparable immunoprecipitation of $FXR2P^{WT}$ and $FXR2P^{G2A}$ (*asterisk*; ~100kD), while neither was detected when a control IgG was used for the immunoprecipitation. Anti-biotin western blotting detected protein that incorporated the myristic analog. $FXR2P^{WT}$ is biotinylated when the click reaction is performed after immunoprecipitation with an FXR2P antibody (*asterisk* marks ~100kD band corresponding to clicked FXR2P). $FXR2P^{G2A}$ is not biotinylated after immunoprecipitation with an FXR2P antibody and click reaction. Equivalent results were observed in four independent experiments.

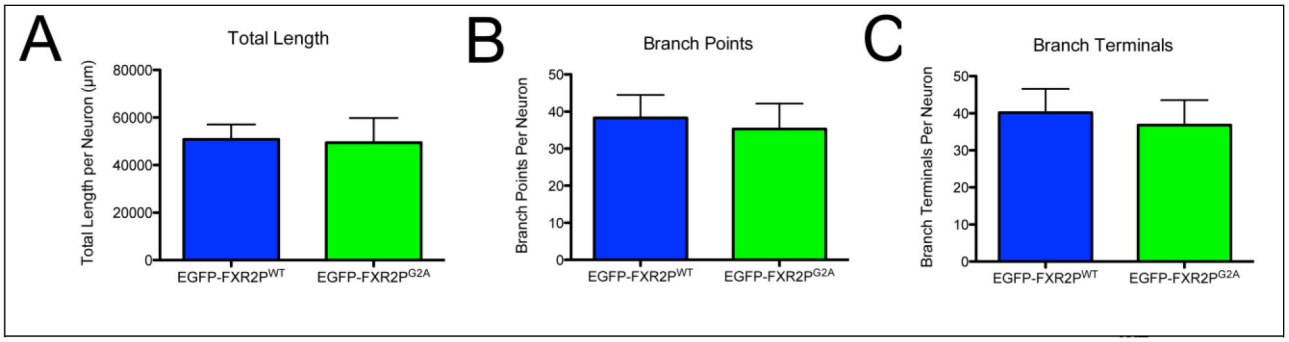


**Figure 2. Comparable axonal arborization in neurons expressing EGFP-FXR2P$^{WT}$ or EGFP-FXR2P$^{G2A}$.**

TdTomato-filled axonal arbors were reconstructed from neurons co-transfected with either EGFP-FXR2P$^{WT}$ or EGFP-FXR2P$^{G2A}$. The average total axon length **(A)**, the number of branch points **(B)** and number of branch terminals **(C)** in neurons expressing EGFP-FXR2P$^{WT}$ or EGFP-FXR2P$^{G2A}$ was similar. n = 6 reconstructed neurons at DIV6 for each condition.

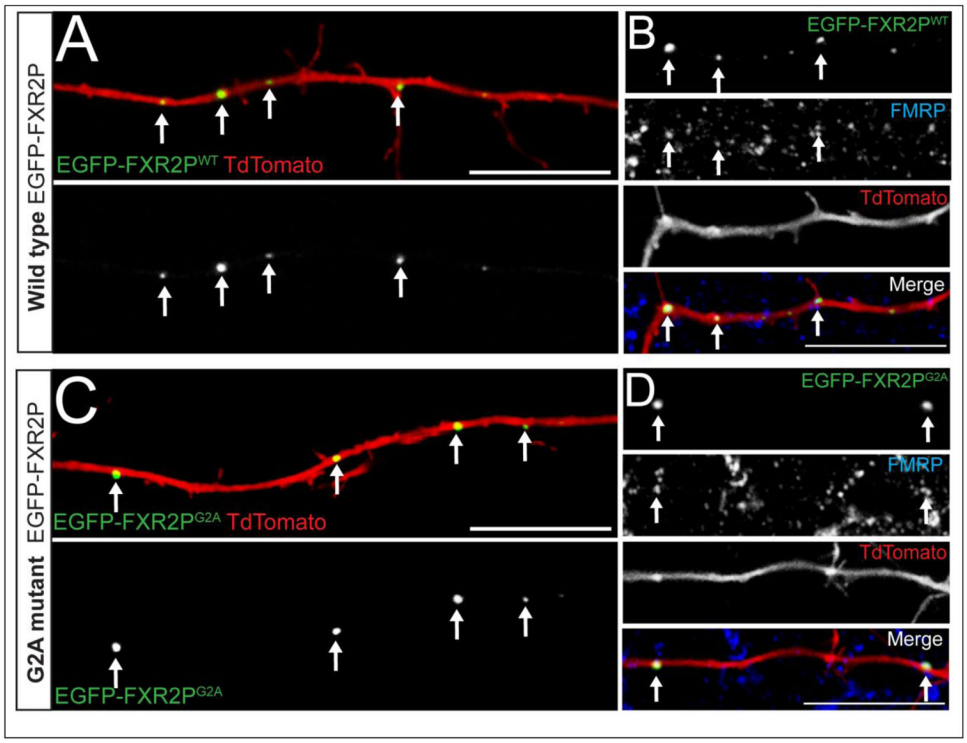


**Figure 3. FXR2P forms granules and associates with FMRP within axons independently of N-myristoylation**

DIV3 cortical neuron cultures were co-transfected with TdTomato (red) along with either wild type (**A, B**) or unmyristoylatable (**C, D**) EGFP-FXR2P (WT or G2A, respectively; green). Note that both wild type and myristoylation-deficient FXR2P are localized to discrete granules (arrows) in the proximal regions of the axon. Axonal granules containing either EGFP-FXR2P$^{WT}$ **(B)** or EGFP-FXR2P$^{G2A}$ **(D)** co-localized with FMRP (blue). DIV6 neurons. Scale bar = 20μm.

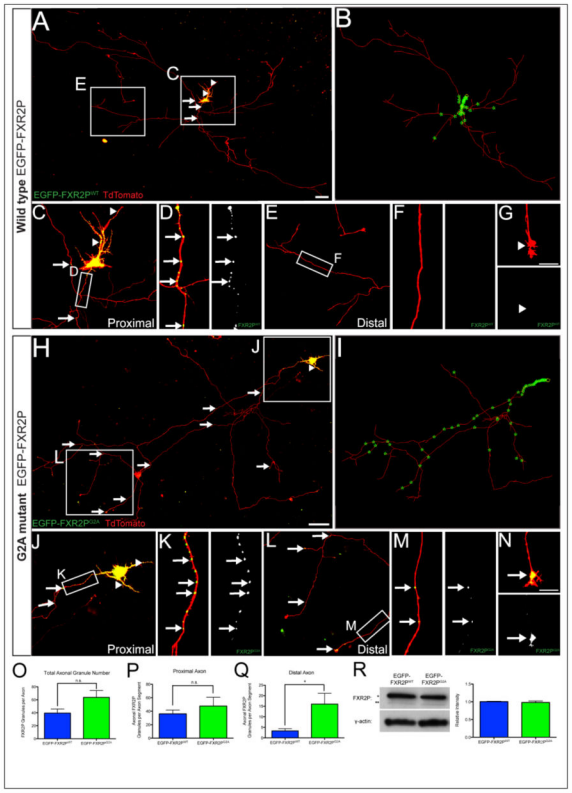


**Figure 4. Differential axonal distribution of wild type and N-myristoylation-deficient FXR2P**

**(A)** The entire axonal arbor of a cortical neuron expressing wild type FXR2P (EGFP-FXR2P$^{WT}$; green) and TdTomato (red). EGFP-FXR2P$^{WT}$ localizes to granules in proximal axon segments (arrows). Granules are also observed in dendrites (arrowheads). **(B)** Neurolucida reconstruction of EGFP-FXR2P$^{WT}$ expressing neuron in A. Green stars mark the location of EGFP-FXR2P$^{WT}$ granules within the axonal arbor (red). **(C, D)** Progressively higher magnifications showing the abundance of EGFP-FXR2P$^{WT}$ granules (arrows) in proximal axon segments. **(E–G)** In contrast EGFP-FXR2P$^{WT}$ granules were rare in distal axon segments or growth cones. **(H)** The entire TdTomato filled axonal arbor of a cortical neuron expressing unmyristoylatable FXR2P (EGFP-FXR2P$^{G2A}$; green). **(I)** Neurolucida reconstruction of EGFP-FXR2P$^{G2A}$ expressing neuron in G. **(J–K)** Progressively higher magnifications of EGFP-FXR2P$^{G2A}$ localization to numerous granules in proximal axonal segments. **(L–M)** Progressively higher magnifications showing that EGFP-FXR2P$^{G2A}$ granules are abundant in distal axonal segments. **(N)** EGFP-FXR2P$^{G2A}$ also localized to growth cones**. (O–Q)** The distribution of FXR2P granules in axons was analyzed using a Sholl analysis with concentric radii of 20 μm extending from the center of the soma and the number of EGFP-FXR2P puncta within each segment was identified and counted. There was no detectable difference in the total number of granules per axon between EGFP-FXR2P$^{WT}$ and EGFP-FXR2P$^{G2A}$ expressing neurons. At proximal axon segments (<2000 μm from cell soma), there was no difference in the total number of axonal granules between EGFP-FXR2P$^{WT}$ and EGFP-FXR2P$^{G2A}$ expressing neurons. The number of axonal FXR2P granules was significantly increased in distal axonal arbors of neurons expressing EGFP-FXR2P$^{G2A}$ compared to EGFP-FXR2P$^{WT}$ (* = $p < 0.05$; n = 6 neurons

per condition). **(R)** Western blot analysis using total protein extracts from neuronal cultures expressing either EGFP-FXR2P$^{WT}$ or EGFP-FXR2P$^{G2A}$ indicates that both were expressed at equivalent levels (FXR2P antibody; n = 3 cultures per condition). Upper band in blot is EGFP-FXR2P (*) while lower band is endogenous FXR2P (**). Actin served as a loading control. DIV6 neurons. Scale bar = 100 μm in A, H; 10 μm in G, N.